Vacuum stability and scalar masses in the superweak extension of the standard model

Zoltán Péli[*]

University of Debrecen and ELKH-DE Particle Physics Research Group, 4010 Debrecen, P.O. Box 105, Hungary

Zoltán Trócsányi[†]

Institute for Theoretical Physics, ELTE Eötvös Loránd University, Pázmány Péter sétány 1/A, 1117 Budapest, Hungary and University of Debrecen and ELKH-DE Particle Physics Research Group, 4010 Debrecen, P.O. Box 105, Hungary

(Received 24 April 2022; accepted 12 September 2022; published 30 September 2022)

We study the allowed parameter space of the scalar sector in the superweak extension of the standard model (SM). The allowed region is defined by the following conditions: (i) stability of the vacuum, (ii) perturbativity up to the Planck scale, and (iii) the pole mass of the Higgs boson falling into its experimentally measured range. We employ renormalization group equations and quantum corrections at two-loop accuracy. We study the dependence on the Yukawa couplings of the sterile neutrinos at selected values. We also check the exclusion limit set by the precise measurement of the mass of the W boson. Our method for constraining the parameter space using two-loop predictions can also be applied to simpler models such as the singlet scalar extension of the SM in a straightforward way.

DOI: 10.1103/PhysRevD.106.055045

I. INTRODUCTION

Currently, particle physics is in a similar situation as physics was about 120 years ago. Its standard model (SM) can successfully explain most of the low and high energy phenomena and provide predictions that are in agreement with measurements at high precision. Nevertheless, there are also a handful of outstanding observations that cannot be predicted by the standard model and that point towards beyond the standard model (BSM) physics. These unexplained facts are (i) the nonvanishing neutrino masses and mixing matrix elements [1,2], (ii) the metastable vacuum of the standard model [3–6], (iii) the need for leptogenesis and/or baryogenesis to explain baryon asymmetry, i.e., our obvious existence, (iv) the existence of dark matter in the Universe [7–11], and also (v) the existence of dark energy in the Universe [7]. In addition, there is general consensus about the occurrence of cosmic inflation in the early Universe, which also calls for an explanation. There are other observations in particle physics that have almost reached discovery status. Most prominently, the prediction of the standard model for the anomalous magnetic moment a_μ of the muon [12] is smaller than the result of the measurement [13,14] by 4.2 standard deviations. In this case, however, the status of the theory is controversial because the evaluation of the hadronic contribution to a_μ requires a nonperturbative approach, and the result depends on the method [12,15]. The resolution of this discrepancy calls for an independent evaluation of this hadronic vacuum polarization contribution before discovery can be claimed.

Some of the observations (i)–(v) should find understanding in particle physics models, while others may have cosmological origins. Nevertheless, the intimate relation between particle physics and the early Universe, originating from the universal expansion of space-time, gives strong support for searching for answers within particle physics by extending the SM. Such extensions can be put into three categories: (a) ultraviolet complete models from theoretical motivations, such as supersymmetric models; (b) effective field theories like the standard model effective field theory (SMEFT); and (c) simplified models that focus on a subset of open questions. This third category includes the dark photon models (gauge extension; see, e.g., Refs. [16,17]), the singlet scalar extensions (see, e.g., Refs. [18–20]), and the introduction of neutrino mass matrices with some variant of the seesaw mechanism, such as in Ref. [21].

[*]zoltanpeli92@gmail.com
[†]zoltan.trocsanyi@cern.ch

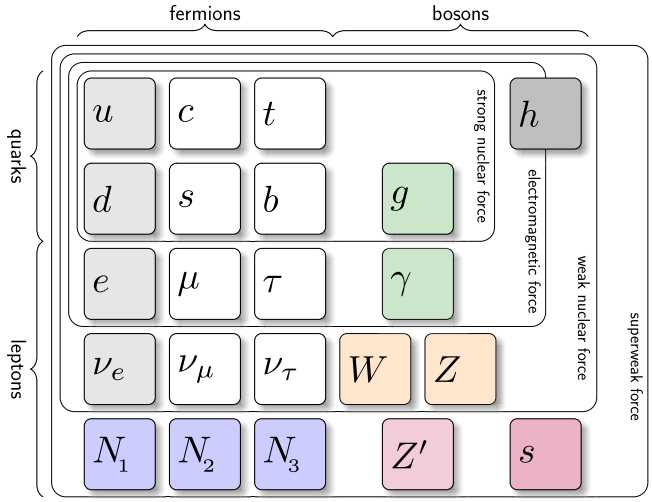

FIG. 1. Standard model particle sheet with the superweak extension. The forces act on all particles within the respective box.

The UV complete supersymmetric extensions of the SM are very attractive for solving theoretical issues, but they are becoming less favored by the results of the LHC experiments [22,23]. Effective field theories have proven to be very useful in the past. However, the SMEFT contains 2499 dimension-six operators [24], which makes it rather difficult to study experimentally. The simplified models on the other end contain only a few new parameters and hence are very attractive from the experimental point of view. However, being simplified models, they cannot give answers to all observations pointing towards BSM physics simultaneously.

In this paper we study a simple UV complete BSM extension along the principles of the SM itself: a renormalizable gauge theory that adds one layer of interactions below the hierarchic layers of the strong, electromagnetic, and weak forces—which is called the superweak (SW) force [25]—mediated by a new U(1) gauge boson Z'; see Fig. 1. In order to explain the origin of neutrino masses, the field content is enhanced by three generations of right-handed neutrinos. The new gauge symmetry is broken spontaneously by the vacuum expectation value of a new complex scalar singlet. According to exploratory studies, the superweak extension of the standard model (SWSM) has the potential to explain the origin of (i) neutrino masses and mixing matrix elements [26], (ii) dark matter [27], (iii) cosmic inflation [28], (iv) stabilization of the electroweak vacuum [28], and possibly (v) leptogenesis (under investigation).

While these findings are promising, more refined analyses are needed in order to explore the viability of the model. The main motivation of our work is not to prove that the SWSM is the correct description of the fundamental interactions but rather to check if questions (i)–(v) listed above can be answered within a single model with as few new parameters as possible. In this paper we revisit the study of the parameter space of the scalar sector of the SWSM as allowed by the requirement of the stability of the vacuum. We improve significantly on our previous analysis [28] in two respects. First, we use renormalization group equations (RGEs) containing the beta functions at two-loop order. More importantly, we take into account both the radiative corrections up to two-loop accuracy and the measured physical values and uncertainties of the parameters of the scalar sector as constraints. A similar study has been performed earlier in the simplified model of a single real scalar extension of the SM in Ref. [20]. The important difference between the present work and that analysis is that we include the effect of the right-handed neutrinos in the running of the couplings, which constrains the parameter space further. For the first time, the inclusion of the two-loop effects is also given in the present work.

II. SUPERWEAK MODEL

The SWSM is a gauged U(1) extension of the standard model with an additional complex scalar field χ and three families of sterile neutrinos $\nu_{\mathrm{R},i}$. The model was defined in Ref. [25], and further details on the new sectors were presented in Refs. [26,28]. Here we recall some details relevant to the present analysis.

The anomaly-free charge assignment is shown in Table I. In particular, the χ field does not couple directly to any fields of the SM.

After spontaneous symmetry breaking (SSB), we parametrize the SM scalar doublet ϕ and the new scalar field as

$$\phi = \frac{1}{\sqrt{2}} \begin{pmatrix} -\mathrm{i}\sqrt{2}\sigma^+ \\ v + H + \mathrm{i}\sigma_\phi \end{pmatrix} \quad \text{and} \quad \chi = \frac{1}{\sqrt{2}}(w + S + \mathrm{i}\sigma_\chi), \tag{1}$$

where v and w are the two vacuum expectation values (VEVs), H and S are two real scalar fields, and σ^+ and $\sigma_{\phi/\chi}$ are charged and neutral Goldstone bosons. In terms of these fields the scalar potential in the SWSM is given by

TABLE I. Group representations and charges of the fermions and scalars in the SWSM.

Field	$\mathrm{SU}(3)_\mathrm{c}$	$\mathrm{SU}(2)_\mathrm{L}$	$\mathrm{U}(1)_Y$	$\mathrm{U}(1)_z$
Q_L	**3**	**2**	$\frac{1}{6}$	$\frac{1}{6}$
u_R	**3**	**1**	$\frac{2}{3}$	$\frac{7}{6}$
d_R	**3**	**1**	$-\frac{1}{3}$	$-\frac{5}{6}$
L_L	**1**	**2**	$-\frac{1}{2}$	$-\frac{1}{2}$
ℓ_R	**1**	**1**	-1	$-\frac{3}{2}$
N_R	**1**	**1**	0	$\frac{1}{2}$
ϕ	**1**	**2**	$\frac{1}{2}$	1
χ	**1**	**1**	0	-1

$$V(\phi,\chi) = V_0 - \mu_\phi^2|\phi|^2 - \mu_\chi^2|\chi|^2 + \lambda_\phi|\phi|^4 + \lambda_\chi|\chi|^4 + \lambda|\phi|^2|\chi|^2. \tag{2}$$

The constant V_0 is irrelevant in our considerations, so we set it to zero in the rest of the paper. Substituting the parametrization (1) into (2), we obtain the tree-level (effective) potential

$$V(H,S) = -\frac{1}{2}(\mu_\phi^2 H^2 + \mu_\chi^2 S^2) + \frac{1}{4}(\lambda_\phi H^4 + \lambda_\chi S^4 + \lambda H^2 S^2) \tag{3}$$

of the real scalar fields. The VEVs are determined by the tadpole equations:

$$\left.\frac{\partial V}{\partial H}\right|_{H=v,S=w} = 0 = v\left(-\mu_\phi^2 + \frac{1}{2}\lambda w^2 + \lambda_\phi v^2\right),$$
$$\left.\frac{\partial V}{\partial S}\right|_{H=v,S=w} = 0 = w\left(-\mu_\chi^2 + \frac{1}{2}\lambda v^2 + \lambda_\chi w^2\right). \tag{4}$$

The mass matrix of the scalar fields is given by the Hessian:

$$\mathbf{M}_\mathrm{s}^2 = \begin{pmatrix} \frac{\partial^2 V}{\partial H^2} & \frac{\partial^2 V}{\partial H \partial S} \\ \frac{\partial^2 V}{\partial S \partial H} & \frac{\partial^2 V}{\partial S^2} \end{pmatrix}_{H=v,S=w} = \begin{pmatrix} 2\lambda_\phi v^2 & \lambda v w \\ \lambda v w & 2\lambda_\chi w^2 \end{pmatrix}, \tag{5}$$

which can be diagonalized by a rotation matrix

$$\mathbf{Z}_\mathrm{s} = \begin{pmatrix} \cos\theta_\mathrm{s} & \sin\theta_\mathrm{s} \\ -\sin\theta_\mathrm{s} & \cos\theta_\mathrm{s} \end{pmatrix}, \tag{6}$$

so that $\mathbf{Z}_\mathrm{s}^T \mathbf{M}_\mathrm{s}^2 \mathbf{Z}_\mathrm{s} = \mathrm{diag}(M_h^2, M_s^2)$. The parameters M_h and M_s are the masses of the propagating states h and s [29]. The positivity condition for the masses implies the condition

$$(4\lambda_\chi\lambda_\phi - \lambda^2) v^2 w^2 > 0 \tag{7}$$

among the scalar couplings and VEVs. Explicitly, the angle of rotation and the scalar masses M_h and M_s can be expressed through the VEVs and couplings at tree level as

$$\tan(2\theta_\mathrm{s}) = \frac{\lambda v w}{\lambda_\chi w^2 - \lambda_\phi v^2}, \tag{8}$$

$$M_h^2 = \lambda_\phi v^2 + \lambda_\chi w^2 - \frac{\lambda_\chi w^2 - \lambda_\phi v^2}{\cos(2\theta_\mathrm{s})}, \tag{9}$$

$$M_s^2 = \lambda_\phi v^2 + \lambda_\chi w^2 + \frac{\lambda_\chi w^2 - \lambda_\phi v^2}{\cos(2\theta_\mathrm{s})}. \tag{10}$$

In the absence of mixing ($\lambda = 0$, $\theta_\mathrm{s} = 0$) we have $M_h = \sqrt{2\lambda_\phi v^2}$, $M_s = \sqrt{2\lambda_\chi w^2}$. As the scalar fields are coupled to the $W^\pm$ bosons with the interaction vertices

$$\Gamma_{hWW}^{\mu\nu} = \frac{\mathrm{i}}{2}(g_\mathrm{L}^2 v\cos\theta_\mathrm{s}) g^{\mu\nu} \quad \text{and} \quad \Gamma_{sWW}^{\mu\nu} = \frac{\mathrm{i}}{2}(g_\mathrm{L}^2 v\sin\theta_\mathrm{s}) g^{\mu\nu}, \tag{11}$$

only the BEH field is coupled to the W bosons and to the other SM fields in the limit of vanishing mixing between the scalars. Hence, we naturally identify the VEV v as that related to the Fermi coupling, and also the parameter M_h with the mass of the Higgs boson measured at the LHC [30], by introducing the notation

$$m_h = 125.10\ \mathrm{GeV}, \qquad \Delta m_h = 0.14\ \mathrm{GeV}, \quad \text{and}$$
$$v = (\sqrt{2}G_\mathrm{F})^{-1/2} = 246.22\ \mathrm{GeV}, \tag{12}$$

and requiring $M_h \in [m_h - \Delta m_h, m_h + \Delta m_h]$. In accordance with this assumption, we restrict θ_s to fall in the range $(-\pi/4, \pi/4)$.

The VEV w can be expressed through these known parameters and the scalar couplings using Eqs. (8) and (9),

$$w = M_h\sqrt{\frac{M_h^2 - 2\lambda_\phi v^2}{2\lambda_\chi(M_h^2 - 2\lambda_\phi v^2) + \lambda^2 v^2}} = \frac{1}{2v}\left|\frac{\sin(2\theta_S)(M_h^2 - M_s^2)}{\lambda}\right|. \tag{13}$$

Thus, the formal conditions for the nonvanishing w, required at the electroweak scale, are either

$$M_h{}^2 > 2\lambda_\phi v^2, \quad \text{with} \quad 4\lambda_\chi\lambda_\phi > \lambda^2 \tag{14}$$

[the second condition deriving from the positivity constraint in (7) for positive $v^2 w^2$], or

$$4\lambda_\chi\left(\lambda_\phi - \frac{1}{2}\frac{M_h^2}{v^2}\right) > \lambda^2, \quad \text{if } 2\lambda_\phi v^2 > M_h{}^2 > 0. \tag{15}$$

As we have fixed v and M_h experimentally, the input value of λ_ϕ decides which of these two cases is to be considered.

Equations (3)–(5) are valid at tree level. The effect of the quantum corrections can be summarized by substituting the potential V with the effective potential V_eff, whose formal loop expansion is

$$V_\mathrm{eff} = \sum_{i=0}^{\infty} V_\mathrm{eff}{}^{(i)} \tag{16}$$

where $V_\mathrm{eff}{}^{(0)} = V$ and $V_\mathrm{eff}{}^{(i)}$ represents the i-loop correction.

III. VACUUM STABILITY IN THE SWSM AT ONE-LOOP ACCURACY

The potential (3) is stable if it is bounded from below. Due to its continuity in the field variables, it is sufficient to study the positivity of (3) for large values of h and s, which translates to the following conditions on the quartic scalar couplings:

$$\lambda_\phi, \lambda_\chi > 0, \qquad 4\lambda_\phi\lambda_\chi - \lambda^2 > 0 \quad \text{for } \lambda < 0. \tag{17}$$

Taking into account the radiative corrections, we get the dependence on the renormalization scale μ for all renormalized couplings, as well as the corrections ${V_{\text{eff}}}^{(i)}$. While it is straightforward to require that the conditions (17) be satisfied for the running couplings at any sensible value of μ, we cannot write the stability conditions for the one-loop effective potential in a closed form such as in Eq. (17) valid at tree level. Hence, we investigate the stability of the potential in Eq. (3) with running couplings.

Nontrivial phenomenology exists if $w > 0$, otherwise there would be no observable mixing in the scalar sector, which can be seen by looking at Eq. (5). Contrary to the stability condition of the effective potential with higher-order quantum corrections, the existence of the new VEV w can be established with high accuracy. We require the existence of a nonvanishing $w(M_\text{t})$ indirectly, extracting it from the known pole mass of the Higgs boson, rather than computing it explicitly from the effective potential (16) with radiative corrections taken into account. Our procedure can be described in terms of analytic expressions at the one-loop accuracy as follows.

We investigate the vacuum stability in the range $\mu \in (M_\text{t}, M_\text{Pl})$, i.e., from the pole mass M_t of the t quark up to the Planck mass M_Pl where quantum gravitational effects become important. The scale dependence of a given coupling g is described by the autonomous system of coupled differential equations of the form

$$\frac{\partial g}{\partial t} = \beta_g, \tag{18}$$

called RGEs, where $\partial/\partial t = \mu\partial/\partial\mu$. We assume that the model remains perturbatively valid for the complete range by requiring

$$|g(\mu)| < 4\pi, \qquad \mu \in (M_\text{t}, M_\text{Pl}) \tag{19}$$

for any coupling g in the theory, which we check in the stability analysis. Consequently, we can employ perturbation theory to compute the β_g functions. We integrate the complete set of RGEs of the SWSM, while requiring the stability and perturbativity conditions (17) and (19). We also assume the existence of w at the scale $\mu = M_\text{t}$, which implies the existence of a second massive neutral gauge boson and a second massive scalar particle as predictions of the model. To check this condition, we compute the loop corrected scalar mixing angle and scalar pole masses:

$$\tan(2\theta_\text{s}(p^2)) = \frac{\lambda(\mu)v(\mu)w(\mu) + \Pi_{HS}(p^2)}{\lambda_\chi(\mu)w(\mu)^2 - \lambda_\phi(\mu)v(\mu)^2 + \Pi_-(p^2)}, \tag{20}$$

$$M_h^2 = \lambda_\phi(\mu)v(\mu)^2 + \lambda_\chi(\mu)w(\mu)^2 + \Pi_+(M_h^2) - \frac{\lambda_\chi(\mu)w(\mu)^2 - \lambda_\phi(\mu)v(\mu)^2 + \Pi_-(M_h^2)}{\cos(2\theta_\text{s}(M_h^2))}, \tag{21}$$

$$M_s^2 = \lambda_\phi(\mu)v(\mu)^2 + \lambda_\chi(\mu)w(\mu)^2 + \Pi_+(M_s^2) + \frac{\lambda_\chi(\mu)w(\mu)^2 - \lambda_\phi(\mu)v(\mu)^2 + \Pi_-(M_s^2)}{\cos(2\theta_\text{s}(M_s^2))}, \tag{22}$$

using the shorthand notation

$$\Pi_\pm(p^2) = \frac{1}{2}(\tilde{\Pi}_{SS}(p^2) \pm \tilde{\Pi}_{HH}(p^2)), \tag{23}$$

where $\tilde{\Pi}_{\varphi\varphi}(p^2) = \Pi_{\varphi\varphi}(p^2) - T_\varphi/\langle\varphi\rangle$, with $\Pi_{\varphi_I\varphi_J}(p^2)$ being the sum of all one-particle-irreducible (1PI) two-point functions with external legs φ_I and φ_J, while T_φ is the sum of all 1PI one-point functions with external leg φ (φ, $\varphi_I = H$ or S). In other words, Eqs. (20)–(22) are valid at any order in perturbation theory. We collect these one- and two-point functions computed at one-loop accuracy in Appendix A. As shown explicitly, each coupling and VEV in Eqs. (20)–(22) depends on the renormalization scale μ, but the pole masses ${M_h}^2$ and ${M_s}^2$ do not depend on this renormalization scale up to the effect of neglected higher-order corrections. An important check of our calculations is the independence of the scalar pole masses M_h and M_s of the renormalization scale μ,

$$\mu\frac{\partial M_h}{\partial\mu} = \mu\frac{\partial M_s}{\partial\mu} = 0. \tag{24}$$

As mentioned, we identify the pole mass M_h, computed in perturbation theory in (21), as the observed Higgs boson mass $m_h \pm \Delta m_h$, which constrains the possible values of $w(M_\text{t})$ severely for a given set of input couplings at $\mu = M_\text{t}$. The lower panels in Fig. 2 show the dependence of $|\Delta M_h|$, with $\Delta M_h = M_h - m_h$, on $w(M_\text{t})$. We see that it falls below the experimental uncertainty Δm_h, represented by the dashed lines, in a fairly narrow range of $w(M_\text{t})$. To find the range of values of the allowed ${w^{(i)}}(M_\text{t})$, with the superscript referring to the accuracy in perturbative order, we solve the two equations

$$M_h(w^{(1)})|_{\mu=M_\text{t}} = m_h \pm \Delta m_h \tag{25}$$

for ${w^{(1)}}(M_\text{t})$ numerically. We consider the two solutions to be physical if they are positive, shown by the vertical lines.

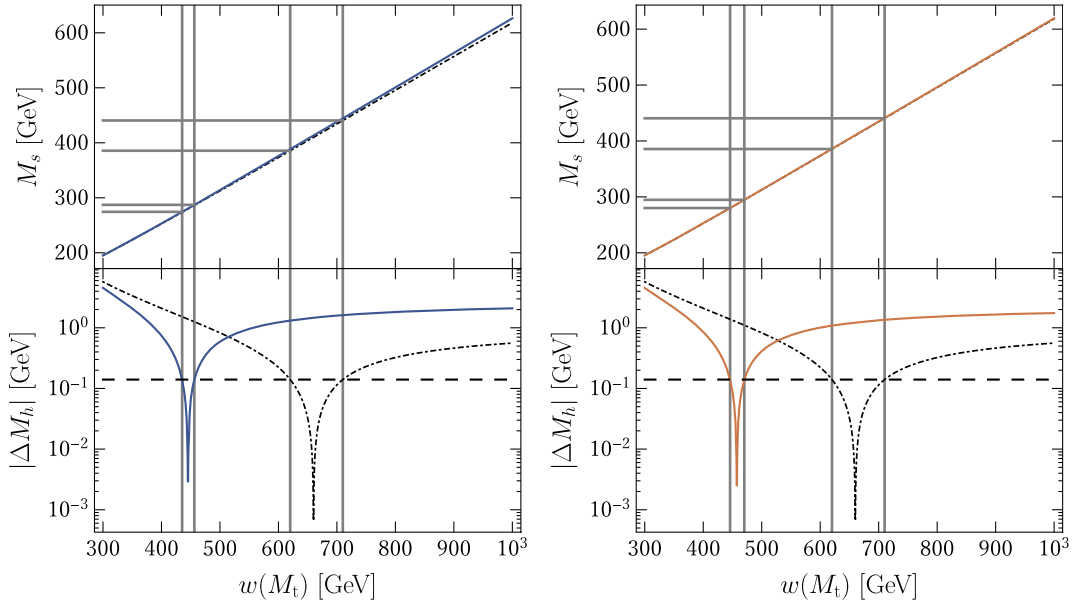

FIG. 2. Dependence of the absolute difference M_h minus the observed Higgs boson mass on $w(M_t)$ (bottom) and the dependence of M_s on $w(M_t)$ (top) with input values $\lambda_\phi(M_t) = 0.15$, $\lambda_\chi(M_t) = 0.2$, and $\lambda(M_t) = 0.1$. Left: $y_x(M_t) = 0$. Right: $y_x(M_t) = 0.8$. The dashed horizontal line corresponds to the uncertainty Δm_h. The black dash-dotted curves are computed at tree level [Eqs. (9) and (10)], while the solid colored ones are computed at one loop [Eqs. (21) and (22)].

Then we use the accepted values $w^{(1)}(M_t)$, falling into the ranges between the vertical line, to compute the possible values of M_s using Eq. (22). This procedure is shown by the plots on the top of Fig. 2 for a specific set of input couplings.

The complete set of running couplings can be grouped into three sets: (i) SM couplings g_Y, g_L, g_s, y_t, (ii) SW gauge coupling g_z, and (iii) scalar quartic couplings $\lambda_\phi, \lambda_\chi, \lambda$, together with the sterile neutrino Yukawa coupling y_x. We assume one light sterile neutrino—a candidate for dark matter [27]—and two heavy ones with equal masses for simplicity, $y_x = y_{x,5} = y_{x,6}$. We neglect the effect of the SW gauge coupling from our analysis because its maximally allowed value is very small, $g_z \lesssim 10^{-4}$, if the model is to explain the origin of dark matter [27] and also obey the direct observational limit of the NA61 experiment [31]. Explicitly, in group (iii) we have the following autonomous system of RGEs at one loop:

$$\begin{aligned}
\frac{\partial\lambda_\phi}{\partial t} &= \beta^{(1)}_{\lambda_\phi,\mathrm{SM}} + \frac{\lambda^2}{(4\pi)^2},\\
\frac{\partial\lambda_\chi}{\partial t} &= \frac{1}{(4\pi)^2}(20\lambda_\chi^2 + 2\lambda^2 - 2y_x^4 + 4\lambda_\chi y_x^2),\\
\frac{\partial\lambda}{\partial t} &= \frac{\lambda}{(4\pi)^2}\left(-\frac{3}{2}g_Y^2 - \frac{9}{2}g_L^2 + 12\lambda_\phi + 8\lambda_\chi + 4\lambda + 6y_t^2 + 2y_x^2\right),
\end{aligned} \tag{26}$$

for the scalar couplings, with $\beta^{(1)}_{\lambda_\phi,\mathrm{SM}}$ being the one-loop beta function of the SM quartic scalar coupling, and

$$\frac{\partial y_x}{\partial t} = \frac{2y_x^3}{(4\pi)^2}, \qquad \frac{\partial w}{\partial t} = -\frac{w}{(4\pi)^2}\frac{y_x^2}{2} \tag{27}$$

for the Yukawa coupling and new VEV. The one-loop beta functions show that a sufficiently large Higgs portal coupling λ is able to drive λ_ϕ and λ_χ to positive values, while the sterile neutrino Yukawa couplings drive λ_χ towards negative values. In the last equation, the RGE for w does not affect the vacuum stability analysis. We present it to check the conditions in Eq. (24).

There are three SM precision parameters measured precisely: G_F, M_Z, and $\alpha_{\mathrm{em}}^{\overline{\mathrm{MS}}}(M_Z)$, which can be turned into input values for the couplings in group (i), together with the less precisely known M_t and $\alpha_s^{\overline{\mathrm{MS}}}(M_Z)$. The self-energies $\Pi_{WW}(p^2)$ and $\Pi_{ZZ}(p^2)$ also receive contributions $\Pi_{VV}^{\mathrm{SW}}(p^2)$ due to the SW extension, given in Eq. (B1), which shift the input values of the VEV v and the electroweak gauge couplings. Hence, we use the following inputs in group (i):

$$\begin{aligned}
g_Y(M_t) &= 0.3586 + \delta g_Y(M_t),\\
g_L(M_t) &= 0.6477 + \delta g_L(M_t),\\
v(M_t) &= 247.55\ \mathrm{GeV} + \delta v(M_t),
\end{aligned} \tag{28}$$

with $g_s(M_t) = 1.167$ and $y_t(M_t) = 0.940$. The SW corrections δg_Y, δg_L, and δv are defined in Appendix B. The SM value of the gauge- and scale-dependent VEV v in the Feynman gauge is $v_{\mathrm{SM}}(M_t) = 247.55$ GeV. The SW corrections to the electroweak input parameters δg_Y, δg_L, and

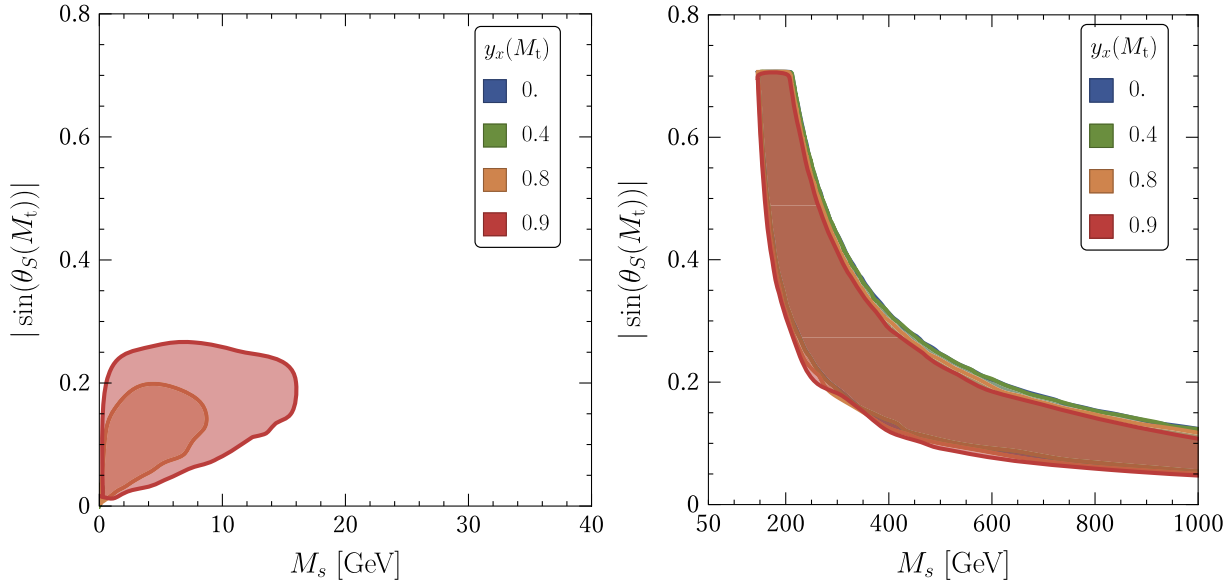

FIG. 3. Allowed parameter space $V_\lambda(y_x)$ in the $M_s - |\sin(\Theta_S)|$ plane at representative values of y_x at one-loop accuracy. The different colored areas correspond to different values of $y_x(M_t)$ as shown in the legends. Left: $M_s < M_h$. Right: $M_s > M_h$.

δv are small and do not noticeably modify our final results even at two loops. We take the value of $y_t(M_t)$ from the fit formula (25) of Ref. [4] as the largest possible value. This choice is the most conservative one concerning the vacuum stability because the main culprit causing the metastable SM vacuum is the large value of the t quark Yukawa coupling $y_t(M_t)$. The last set (iii) of the input couplings are unconstrained, and we scan their values at $\mu = M_t$ in order to obtain the parameter space in $\{\lambda_\phi, \lambda_\chi, \lambda, y_x\}_{\mu=M_t}$ where the stability (17) and perturbativity (19) conditions in the range $\mu \in (M_t, M_{Pl})$, together with the existence of the w vacuum at $\mu = M_t$, are fulfilled.

We scan the volume $V_\lambda(y_x) = \{\lambda_\phi, \lambda_\chi, \lambda\}_{\mu=M_t}$ spanned by the input couplings at fixed values of $y_x(M_t)$ to find the parameter space allowed by our conditions. There are two quantitatively different regions. In the first one, (a) $M_s < M_h$; i.e., the new scalar is lighter than the Higgs boson. In the second one, (b) $M_s > M_h$. We present the result of such scans in the next section where the computations are performed at two-loop accuracy. Having found the allowed region of the input parameters, we can compute the scalar mixing angle and mass of the new scalar using Eqs. (20) and (22), to obtain the allowed parameter space in the $M_s - |\sin(\theta_s(M_t))|$ plane, shown in Fig. 3 at selected values of the neutrino Yukawa coupling. In case (a), the parameter space is empty for $y_x(M_t) = 0$, but it grows nonlinearly with increasing $y_x(M_t)$. For instance, the parameter space for $y_x(M_t) = 0.4$ is not empty, but it is still invisible at the resolution of Fig. 3, as in that case, one has $M_s < 300$ MeV and $|\sin(\theta_s)| < 0.04$. For $y_x(M_t) \gtrsim 1$, the stability condition $\lambda_\chi > 0$ is not satisfied at any scale below M_{Pl}. It turns out that in case (b) the value of the VEV $w^{(1)}(M_t)$ and hence that of M_s can be larger than shown in the plot when the scalar mixing coupling tends to zero. As that also means vanishing mixing coupling λ, it represents the phenomenologically rather irrelevant case of a very weakly coupled dark sector.

IV. VACUUM STABILITY IN THE SWSM AT TWO-LOOP ACCURACY

In order to check the robustness of the perturbative analysis of the parameter space where the vacuum is stable, we repeat the procedure described in the previous

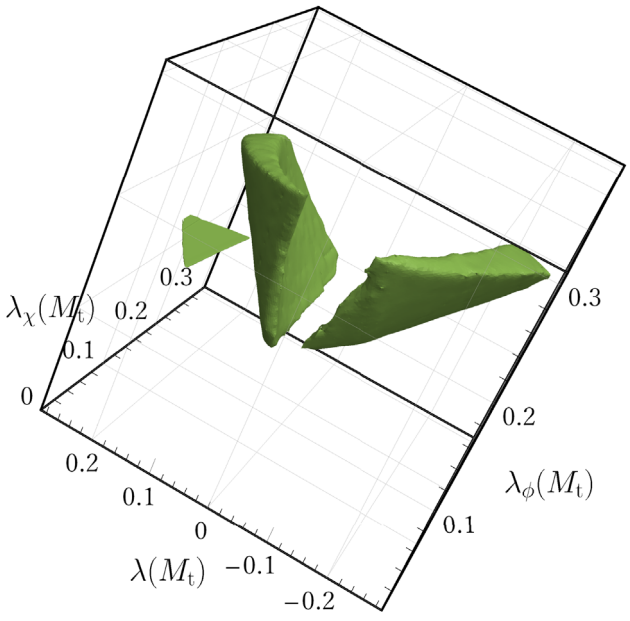

FIG. 4. Three-dimensional parameter space at $y_x(M_t) = 0.4$.

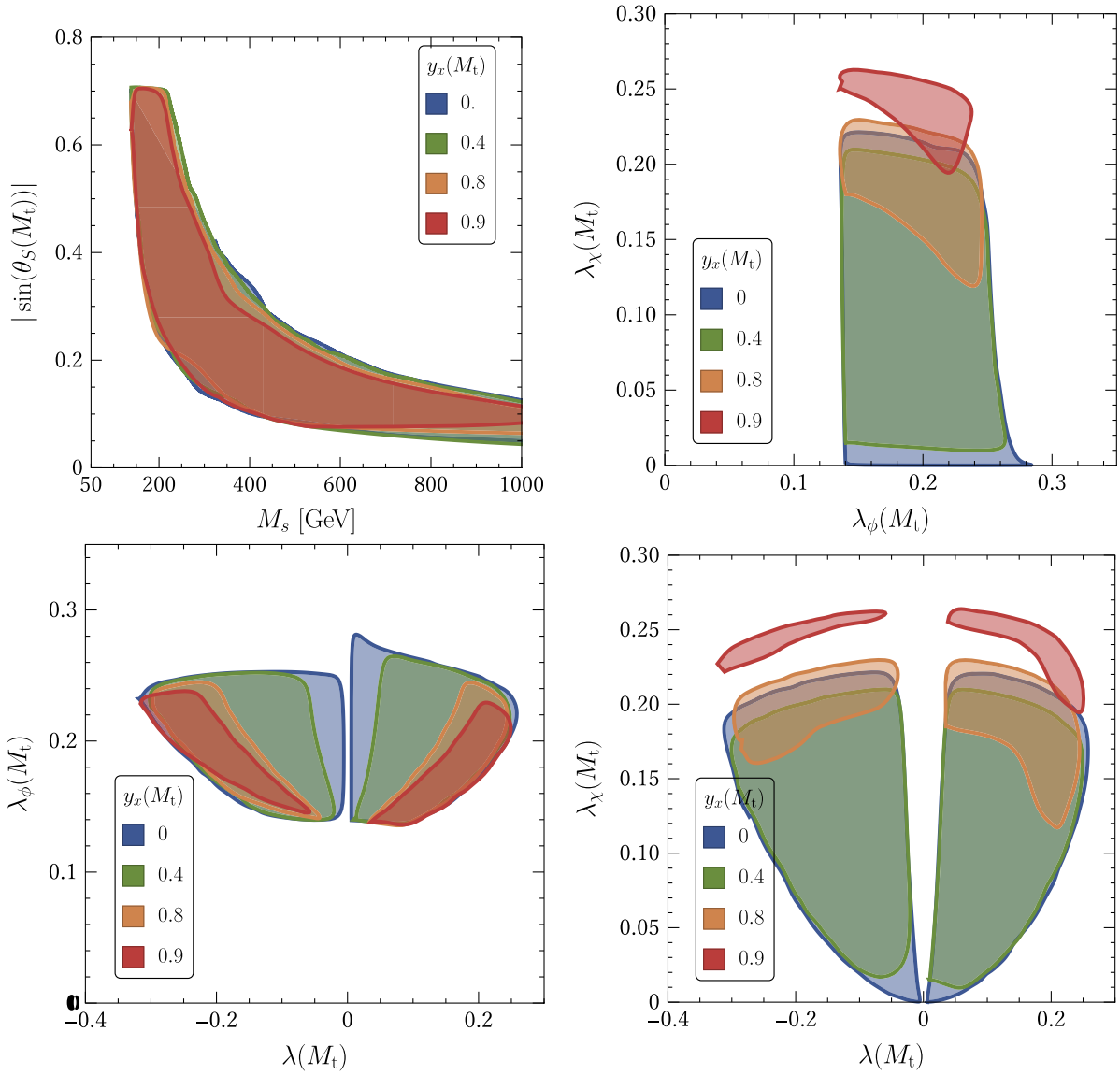

FIG. 5. Planar projections of the allowed parameter space, where $M_s > M_h$ and the conditions (17), (19), $w^{(2)}(M_t) > 0$ are fulfilled at two-loop accuracy. Top left: allowed regions in the $M_s - |\sin\theta_s|$ plane. Other plots show the two-dimensional projections of the three-dimensional allowed regions in $V_\lambda(y_x)$. The different colored regions correspond to different values of y_x as shown in the legends.

section at two-loop accuracy. Given a set of input couplings $\{\lambda_\phi(M_t), \lambda_\chi(M_t), \lambda(M_t), y_x(M_t)\}$, we first compute $w^{(1)}(M_t)$ at $\mu = M_t$, using our analytic formulas as described in the previous section. We solve the two-loop β-functions to check the conditions of stability and perturbativity only if we find $w^{(1)}(M_t) > 0$. If all the stability and perturbativity conditions are fulfilled for the input values $\{\lambda_\phi(M_t), \lambda_\chi(M_t), \lambda(M_t), y_x(M_t)\}$, we use SPheno [32,33] to compute the scalar pole masses at two loops, ${M_h}^{(2)}$ and ${M_s}^{(2)}$, using w as a free input parameter. Starting from the initial value $w = w^{(1)}(M_t)$, we search for the w at which

$$ {M_h}^{(2)}(w) = m_h, \tag{29} $$

which we call $w = w^{(2)}$. This procedure of using only such points in the parameter space where the condition $w^{(1)}(M_t) > 0$ is satisfied saves significant CPU time as the numerical solutions of the two-loop β-functions, and especially the computations in SPheno, are very time-consuming [34].

The parameter space is shown by a perspective view at $y_x(M_t) = 0.4$ in Fig. 4, and its projections to the two-dimensional subspaces at selected values of $y_x(M_t)$ are given in Figs. 5 and 6. We also compute the regions $V_\lambda(y_x)$ using the tree-level relation (13) instead of the one-loop one in Eq. (21) as typically done in the case of scalar singlet extensions (see, e.g., Ref. [35]). We find that the allowed region on the $M_s - |\sin(\theta_s)|$ plane for case (a) $M_s < M_h$ is sensitive to such a change in an interesting way: For a

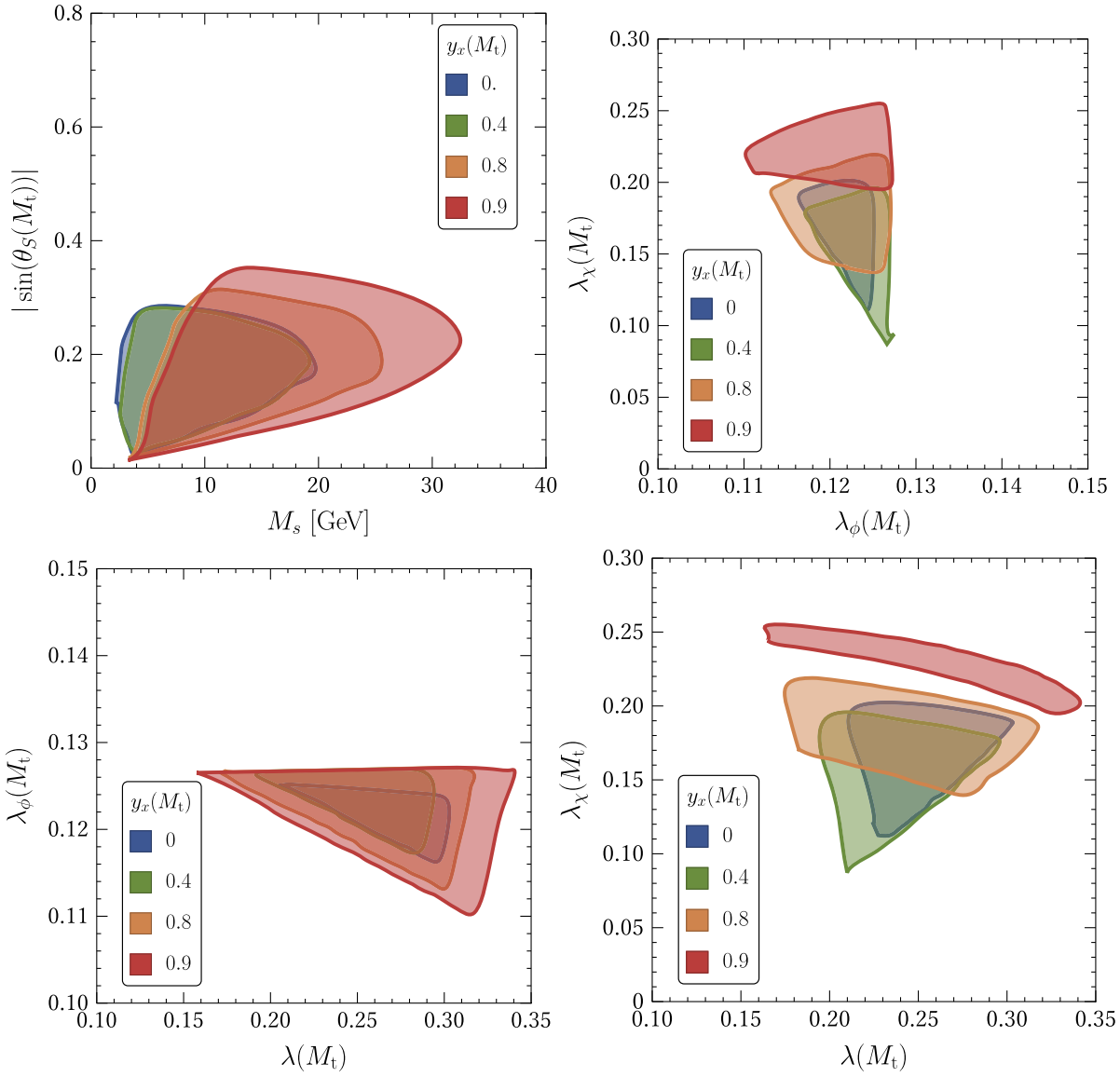

FIG. 6. Same as Fig. 5 but for $M_s < M_h$.

vanishing Yukawa coupling, the allowed region found using Eq. (13) disappears at one loop (see the discussion of Fig. 3 in the previous section) but reappears at two loops, which had not been found in previous analyses. If $y_x(M_t)$ is increased from zero, we find nonempty parameter space at any of the first three orders in perturbation theory. The minimum value of M_s in region (a) depends on $y_x(M_t)$, but it is always larger than about 1 GeV in the two-loop analysis.

One can make two important remarks about the parameter space in case (b) $M_s > M_h$ presented in Fig. 6. On the one hand, the parameter space shrinks as $y_x(M_t)$ increases, and it disappears completely for $y_x(M_t) \gtrsim 1$. On the other hand, we have $|\lambda(M_t)| > 0$ because for $\lambda(M_t) = 0$ the scalar mixing vanishes; then λ_ϕ coincides with $\lambda_{\rm SM}$, which does not satisfy the vacuum stability conditions, while preserving the pole mass of the Higgs boson. Also, the volume $V_\lambda(y_x)$ increases slightly with increasing order in perturbation theory.

We have checked Eq. (24) numerically for both cases (a) and (b) at randomly selected input values $\{\lambda_\phi, \lambda_\chi, \lambda, y_x\}_{\mu=M_t}$ in the range $\mu \in (0.5M_t, 2M_t)$ and compared the scale dependence of the tree-level masses (9) and (10) to the scale dependence of the one-loop accurate pole masses (21) and (22). As shown in Fig. 7, we find that the scale dependence of the tree-level masses is reduced significantly at one-loop and even more at two-loop accuracy. The sizable difference between the scalar pole masses M_s at the first two orders of perturbation theory (and to a much less extent between the next two orders) is not caused by radiative corrections. Rather than loop corrections to the masses, the jumps originate from the shifts in $w(M_t)$ required to reproduce the

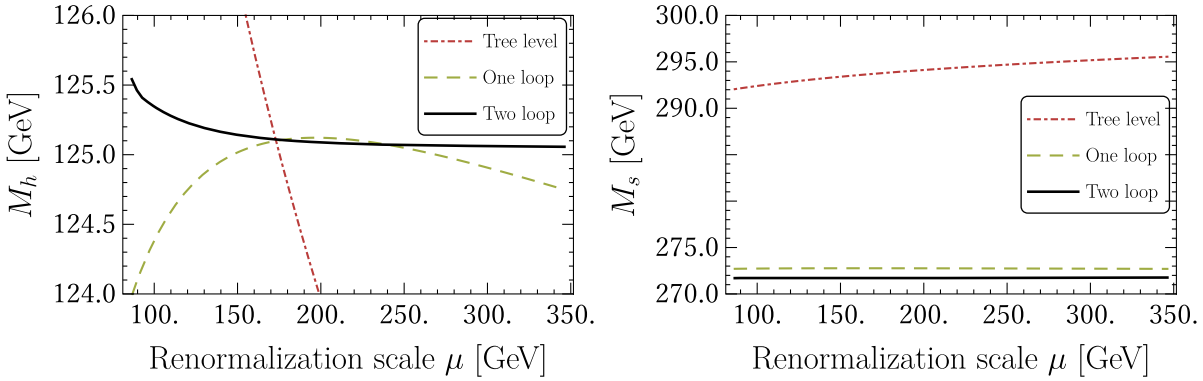

FIG. 7. Dependence of the scalar boson masses $M_h^{(i)}$ and M_s on the renormalization scale μ in the range $(0.5M_t, 2M_t)$ at different orders of perturbation theory at $y_x(M_t) = 0.4$, $\lambda_\phi(M_t) = 0.241$, $\lambda_\chi(M_t) = 0.096$, $\lambda(M_t) = 0.217$.

Higgs boson pole mass at different orders of perturbation theory, as can be seen in Fig. 2.

V. EXPERIMENTAL CONSTRAINTS

The electroweak precision observables (EWPO) [36] are sensitive to BSM physics, such as the existence of an additional scalar particle. Previous analyses show that amongst the EWPO, the W-boson mass is perhaps the most sensitive to a new scalar sector [37,38]. In this work we only consider the mass of the W boson from the EWPO to set exclusion bands on the parameter space [39]. The theoretical prediction for the W-boson mass uses precision electroweak observables (except M_W itself), and it is sensitive to new physics [37]. Hence, it is often used as a benchmark compared to the experimentally observed value [30]

$$M_W^{\rm exp} = 80.379 \pm 0.012 \text{ GeV}. \tag{30}$$

The current, most precise theoretical estimates are $M_W^{\rm theo} = 80.359 \pm 0.011$ GeV [40], 80.362 ± 0.007 GeV [41], and $80.357 \pm 0.009 \pm 0.003$ GeV [42]. We take 80.360 GeV as the SM prediction and the combined uncertainty from the experimental and theoretical values to be $\Delta M_W \simeq 17$ MeV. We set twice this value as an upper limit to find the allowed range for the new physics contribution to $M_W^{\rm theo}$, which means that the SW contribution to the mass of the W boson is excluded outside the range (19 ± 34) MeV, i.e., outside $[-15, 53]$ MeV.

We compute the SW contributions $\delta M_W^{\rm SW}$ to $M_W^{\rm theo}$ at one-loop accuracy. We find that the contribution of the new gauge sector is heavily suppressed due to the required smallness of the new gauge coupling $g_z \lesssim 10^{-4}$. The sterile neutrinos may change the measured value of the Fermi coupling G_F affecting the mass of the W boson already at tree level [43]. In fact, right-handed neutrinos can provide a significant contribution to the W-boson mass [44], although at the price of introducing some tension with universality bounds. Hence, a proper account of the effect of sterile neutrinos is certainly warranted; however, it is beyond the scope of the present paper, and we leave it for a planned global scan of the parameter space. The contribution of the new scalar sector to M_W, however, can be comparable to ΔM_W [37,45]. We present the SW correction δM_W in (B7) of Appendix B, expressed with two free parameters, M_s and $\sin^2\theta_s$. For the case of a light new scalar, $M_s < M_h$, the SW correction is positive, while for the heavy one, it is negative. The excluded regions obtained by (a) $\delta M_W > 53$ MeV and (b) $\delta M_W < -15$ MeV are presented in Fig. 9 together with other experimental constraints that we discuss below. We see that the W-mass measurement at present uncertainties does not provide a significant reduction of the parameter space. However, if the improved measurement published recently by the CDF Collaboration [46] is confirmed, in the high-mass region the stability of the vacuum and the experimental value of the mass of the W boson will become incompatible, as in that case the SW correction to the SM value is negative. The low-mass region also becomes significantly constrained.

In Fig. 8 we present the allowed parameter space, together with contour lines representing the border of the excluded parameter space (below the line), assuming a δM_W increase of the W mass by selected benchmark values due to the new scalar in the self-energy loop [47]. Clearly, the large positive shift required to explain the CDF-II result is not compatible with the conditions of stability and perturbativity of the scalar sector of the model.

The Higgs boson couplings to the SM particles are modified due to the mixing in the extended scalar sector of the SWSM. Consequently, the theoretical predictions for the production and decay rates of the Higgs boson are affected, which can be used to impose exclusion bounds on the parameter space. In the SWSM, the SM Higgs couplings are multiplied by a factor of $\cos\theta_s$. In addition, new decay channels open up:

$$\Gamma(h \to ss) = \frac{\Gamma_{hss}^2}{32\pi M_h^2}\sqrt{1 - 4\frac{M_s^2}{M_h^2}}, \tag{31}$$

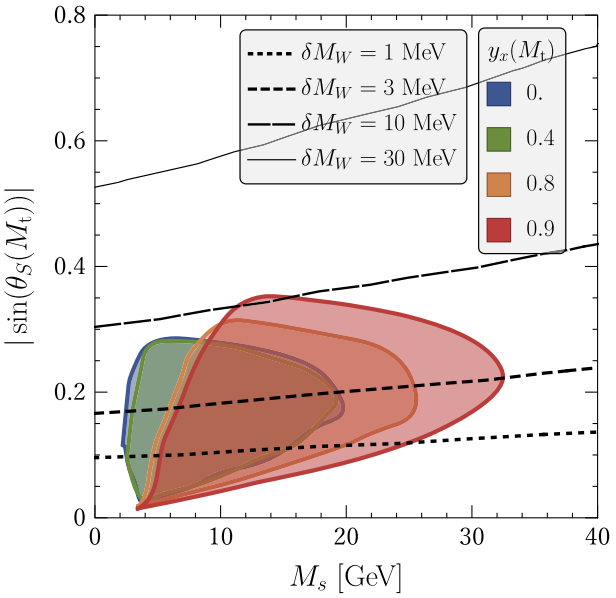

FIG. 8. Allowed parameter space in the $M_s - |\sin(\Theta_S)|$ plane at representative values of y_x at two-loop accuracy for $M_s > M_h$. The contours at selective values of δM_W represent the borderline in the parameter space below which the new scalar cannot be solely responsible for the increase of the W-boson mass by δM_W with respect to the SM value.

$$\Gamma(h \to NN) = \frac{G_F M_h M_N^2}{8\sqrt{2}\pi}\Gamma_{hNN}^2\left(1 - 4\frac{M_N^2}{M_h^2}\right)^{3/2}, \quad (32)$$

when kinematically allowed, with

$$\Gamma_{hss} = \frac{1}{2}\sin(2\theta_S)(M_h^2 + 2M_s^2)\left(\frac{\cos\theta_s}{w} - \frac{\sin\theta_s}{v}\right), \quad (33)$$

$$\Gamma_{hNN} = \sin\theta_s \frac{v}{w} \quad \text{and} \quad M_N = \frac{y_x}{\sqrt{2}}w. \quad (34)$$

In the stability analysis (see Figs. 5 and 6), we find a well-defined parameter space for $M_s < M_h$, with $\theta_S < 0$ and $\lambda \in (0.15, 0.30)$. Thus, it is well motivated to investigate whether the magnitude of the partial width $\Gamma(h \to ss)$ is compatible with the experimental bound on the Higgs boson total width $\Gamma_h = 3.2^{+2.8}_{-2.2}$ MeV [30].

The Γ_{hss} coupling expanded in the limits $M_s \ll M_h$ and $|\theta_S| \ll 1$ yields

$$\Gamma_{hss} \simeq \mathrm{sgn}(\theta_S)\lambda v\left(1 + 3\frac{M_s^2}{M_h^2}\right) - \frac{M_h^2}{v}\theta_S^2\left(1 + 2\frac{M_s^2}{M_h^2}\right). \quad (35)$$

Thus, the estimate for the minimal value of the partial width is

$$\Gamma(h \to ss) = \lambda^2\frac{v^2}{32\pi M_h} \simeq \lambda^2 \times (4.82\ \text{GeV}) \quad (36)$$

for $\theta_S < 0$ and $\lambda > 0$. Near the kinematic threshold where $M_s = \frac{M_h}{2}(1 - \varepsilon)$, one obtains

$$\Gamma(h \to ss) = \lambda^2\frac{v^2}{4\pi M_h}\sqrt{\varepsilon} \simeq \lambda^2 \times (3.44\ \text{GeV})\sqrt{\varepsilon}, \quad (37)$$

with $\varepsilon \ll 1$. This shows that the $\lambda(M_t)$ values allowed in the stability analysis (Figs. 5 and 6) for $M_s < M_h$ are

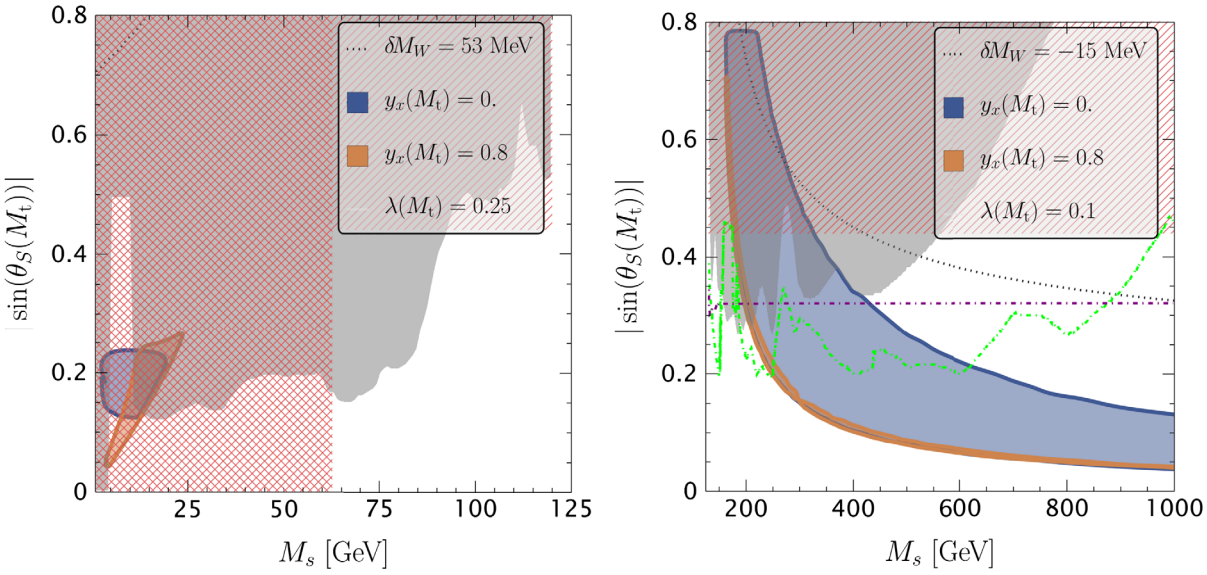

FIG. 9. Allowed parameter space in the $M_s - |\sin(\Theta_S)|$ plane at representative values of y_x and λ. The gray area and the region above the green line correspond to the excluded region by direct searches. The red dashed area and the region above the purple line are excluded by Higgs signal rate measurements [20,38]. The region $M_s < m_h/2$ with the red grid is excluded due to the constraint on the Higgs boson width at $\lambda(M_t) = 0.25$.

incompatible with the experimental bound on the Higgs decay width unless the new scalar mass is very close to $M_h/2$. Clearly, if sterile neutrinos are present, the total width of the Higgs is further increased; thus, we consider the region $M_s < m_h/2$ to be excluded.

The SWSM also contains an additional neutral gauge boson Z', which affects the SM couplings and opens new production and decay channels. We neglect the superweak gauge couplings and the effect of Z' completely in order to focus only on the effect of the extended scalar sector and sterile neutrinos [49].

In this work we do not compute the most up-to-date exclusion bounds set by direct searches; however, we adapt the exclusion from precision tests and Higgs boson coupling measurements from [20] and also from the more recent Ref. [38] for the case of $M_s > M_h$ in order to compare our theoretical predictions with experimental data. We summarize our findings in Fig. 9 at selected values of $\lambda(M_t)$ and $y_x(M_t)$ compared to the W mass and Higgs width restrictions computed by us and the direct search with signal strength measurement restrictions taken from the literature. We show slices of the parameter space taken at different values of $\lambda(M_t)$ with the exclusion limits taken from Refs. [20,38]. However, those works marginalized the dependence on $\lambda(M_t)$ [50].

VI. CONCLUSIONS AND OUTLOOK

In this paper we have scanned the parameter space of the superweak extension of the standard model in order to find the allowed parameter space of the scalar sector where the following assumptions are fulfilled: (i) The vacuum must be stable, (ii) the model parameters must remain perturbative up to the Planck scale, and (iii) the pole mass of the Higgs boson must fall into its experimentally measured range. The first two of these constraints were taken into account in our preliminary work [28]. In this paper we supersede that former study by taking into account the two-loop corrections, both in the renormalization group equations of the running couplings and in the measured value of the mass of the Higgs boson. We have taken into account the largest neutrino Yukawa coupling y_x. In the limit of vanishing y_x and neglecting the superweak gauge coupling, the model essentially reduces to the case of a singlet scalar extension of the standard model.

In the two-loop analysis, we found a nonempty region in the $M_s - \sin\theta_s$ parameter space for $M_s < M_h$, increasing with y_x up to $y_x(M_t) \simeq 1$, where the condition of stability is not fulfilled any longer. Such a region has been missed in the case of $y_x = 0$ in earlier analyses of the singlet scalar extension performed only at one-loop accuracy (see, e.g., Ref. [20]).

Of course, there are many experimental results that also constrain the parameter space. The new physics contributions to electroweak precision observables, as well as direct searches for the decay of a scalar particle into standard model ones, provide strong constraints. Of those, we have studied only the effect of the experimental result on the mass of the W boson in this paper. We have seen that while M_W can indeed limit the parameter space, the current world average without the new CDF-II result cannot provide a further constraint on the parameter space. If we also include the CDF II result in the average—in spite of being incompatible with the previous average—then the parameter space allowed by our assumptions becomes incompatible with the W-mass constraint. We have also included the experimental constraints adopted from Refs. [20,38] for the singlet scalar extension of the standard model, as well as the limit obtained from the measured value of the width of the Higgs boson. As in the SWSM the allowed regions also depend on the Yukawa couplings of the right-handed neutrinos, it will also be important to take into account all the available experimental constraints, not only from collider experiments but also from neutrino experiments. It will also be interesting to check whether possible signatures of the production of a new scalar boson at the LHC (such as those proposed in Refs. [51,52]) can be explained in the SWSM. Such a complete study of the parameter space and searches for signatures is beyond the scope of the present paper, and we leave it to an upcoming study where we plan to use the analytic expressions of the present work.

ACKNOWLEDGMENTS

We are grateful for useful discussions with members of the ELTE PPPhenogroup, especially Josu Hernandez-Garcia, and also Tania Robens at the Munich Institute for Astro-, Particle and BioPhysics (MIAPbP), which is funded by the Deutsche Forschungsgemeinschaft (DFG, German Research Foundation) under Germany's Excellence Strategy—EXC-2094–390783311. This work was supported by Grant No. K 125105 of the National Research, Development and Innovation Fund in Hungary.

APPENDIX A: LOOP CORRECTIONS TO THE SCALAR MASSES IN THE SWSM

On one hand, the quantum effects correct the tadpole equations (4), such that

$$0 = v\left(-\mu_\phi^2 + \frac{1}{2}\lambda w^2 + \lambda_\phi v^2\right) + T_H,$$
$$0 = w\left(-\mu_\chi^2 + \frac{1}{2}\lambda v^2 + \lambda_\chi w^2\right) + T_S, \tag{A1}$$

where T_φ is the sum of all 1PI one-point functions with external leg $\varphi = H$ or S. On the other hand, the scalar self-energies $\Pi_{\varphi_I\varphi_J}$—i.e., the sum of all 1PI Feynman graphs with external legs φ_I and φ_J—directly correct the propagator matrix of the scalar fields H and S. The inverse-propagator matrix, after applying the tadpole equations (A1) to eliminate the mass parameters μ_ϕ and μ_χ, is given as

$$\begin{pmatrix} p^2 & 0 \\ 0 & p^2 \end{pmatrix} - \begin{pmatrix} 2\lambda_\phi v^2 + \tilde{\Pi}_{HH}(p^2) & \lambda v w + \Pi_{SH}(p^2) \\ \lambda v w + \Pi_{HS}(p^2) & 2\lambda_\chi w^2 + \tilde{\Pi}_{SS}(p^2) \end{pmatrix}, \tag{A2}$$

where $\tilde{\Pi}_{\varphi\varphi}(p^2) = \Pi_{\varphi\varphi}(p^2) - T_\varphi/\langle\varphi\rangle$, with $\langle\varphi\rangle = v, w$. In order to obtain the mixing angle θ_s (20) and the scalar pole masses (21) and (22), one has to diagonalize the real part of (A2), leading to Eqs. (20)–(22).

We implement a SARAH model file for the SWSM [26] and use it to compute the one-loop scalar self-energies and tadpoles in Feynman gauge ($\xi = 1$). In the following, we list explicitly the one-loop corrections to the scalar inverse-propagator matrix (A2), after some simplifications of the SARAH output.

The Higgs self-energy is

$$\begin{aligned}
\tilde{\Pi}_{HH}(p^2) = \kappa\Big\{ & 3y_t^2(4m_t^2 - p^2)B_0(p^2, m_t^2, m_t^2) - \frac{1}{2}\lambda^2 v^2 B_0(p^2, 0, 0) + \frac{\lambda w \sin(2\theta_s)}{2v}(A_0(m_s^2) - A_0(m_h^2)) \\
& - \frac{1}{2}(6\lambda_\phi v\cos^2\theta_s - \lambda w \sin(2\theta_s) + \lambda v\sin^2\theta_s)^2 B_0(p^2, m_h^2, m_h^2) \\
& - \frac{1}{2}(\lambda v\cos^2\theta_s + \lambda w \sin(2\theta_s) + 6\lambda_\phi v\sin^2\theta_s)^2 B_0(p^2, m_s^2, m_s^2) \\
& - \frac{1}{2}(\lambda w \cos(2\theta_s) + (3\lambda_\phi - \lambda/2)v \sin(2\theta_s))^2 B_0(p^2, m_s^2, m_h^2) \\
& + \frac{1}{v^2}((4p^2 m_W^2 - 12m_W^4 - 4\lambda_\phi^2 v^4)B_0(p^2, m_W^2, m_W^2) + 8m_W^2) \\
& + \frac{1}{2v^2}((4p^2 m_Z^2 - 12m_Z^4 - 4\lambda_\phi^2 v^4)B_0(p^2, m_Z^2, m_Z^2) + 8m_Z^2)\Big\}
\end{aligned} \tag{A3}$$

where $\kappa = (4\pi)^{-2}$ and $m_p(\mu)$ is the running mass of particle p as computed using tree-level relations. If the elements of the Dirac neutrino mass matrix $\mathbf{M}_D$ are much smaller than those of the Majorana neutrino mass matrix $\mathbf{M}_N$, i.e., $(\mathbf{M}_D)_{ij} \ll (\mathbf{M}_N)_{kk}$ for any $i, j, k \in (1, 2, 3)$, then the loop correction to the scalar mass from the active neutrinos is negligible and the sterile neutrinos contribute to $\tilde{\Pi}_{SS}$ only, namely,

$$\begin{aligned}
\tilde{\Pi}_{SS}(p^2) = \kappa\Big\{ & \frac{1}{2}\sum_{i=1}^{3} y_{x,i}^2(4m_{N,i}^2 - p^2)B_0(p^2, m_{N,i}^2, m_{N,i}^2) + \frac{\lambda v \sin(2\theta_s)}{2w}(A_0(m_s^2) - A_0(m_h^2)) \\
& - \frac{1}{2}(\lambda w\cos^2\theta_s - \lambda v \sin(2\theta_s) + 6\lambda_\chi w\sin^2\theta_s)^2 B_0(p^2, m_h^2, m_h^2) \\
& - \frac{1}{2}(6\lambda_\chi w\cos^2\theta_s + \lambda v \sin(2\theta_s) + \lambda w\sin^2\theta_s)^2 B_0(p^2, m_s^2, m_s^2) \\
& - \frac{1}{2}(\lambda v \cos(2\theta_s) - (3\lambda_\chi - \lambda/2)w \sin(2\theta_s))^2 B_0(p^2, m_s^2, m_h^2) \\
& - w^2\left(\lambda^2 B_0(p^2, m_W^2, m_W^2) + \frac{1}{2}\lambda^2 B_0(p^2, m_Z^2, m_Z^2) - 2\lambda_\chi^2 B_0(p^2, 0, 0)\right)\Big\}
\end{aligned} \tag{A4}$$

and

$$\begin{aligned}
\Pi_{HS}(p^2) = \Pi_{SH}(p^2) = \kappa\Big\{ & \frac{1}{2}\lambda \sin(2\theta_s)(A_0(m_h^2) - A_0(m_s^2)) + \frac{1}{2}(6\lambda_\phi v\cos^2\theta_s - \lambda w \sin(2\theta_s) + \lambda v\sin^2\theta_s) \\
& \times (\lambda w\cos^2\theta_s - \lambda v \sin(2\theta_s) + 6\lambda_\chi w\sin^2\theta_s)B_0(p^2, m_h^2, m_h^2) - \frac{1}{2}(6\lambda_\chi w\cos^2\theta_s + \lambda v \sin(2\theta_s) + \lambda w\sin^2\theta_s) \\
& \times (\lambda v\cos^2\theta_s + \lambda w \sin(2\theta_s) + 6\lambda_\phi w\sin^2\theta_s)B_0(p^2, m_s^2, m_s^2) \\
& - \frac{1}{4}(2\lambda v \cos(2\theta_s) - (6\lambda_\chi - \lambda)w \sin(2\theta_s)) \times (2\lambda w \cos(2\theta_s) + (6\lambda_\phi - \lambda)v \sin(2\theta_s))B_0(p^2, m_s^2, m_h^2) \\
& - \lambda v w(2\lambda_\phi B_0(p^2, M_W^2, M_W^2) + \lambda_\phi B_0(p^2, M_Z^2, M_Z^2) + \lambda_\chi B_0(p^2, M_{Z'}^2, M_{Z'}^2))\Big\}.
\end{aligned} \tag{A5}$$

We have neglected terms proportional to g_z and the mass M'_Z of the Z' boson as $M_{Z'} \ll v, w$. Each coupling and mass in the one-loop contributions (A3)–(A5) is the running parameter depending on the renormalization scale μ, and the vacuum expectation values v and w are the gauge- and scale-dependent running VEVs. We suppress the scale dependence for easier reading. The masses m_x correspond to the tree-level formulas but with running couplings

$$m_t = \frac{1}{\sqrt{2}} y_t v, \qquad m_W = \frac{1}{2} g_{\mathrm{L}} v,$$
$$m_Z = \frac{1}{2}\sqrt{g_Y^2 + g_{\mathrm{L}}^2}\, v, \quad \text{and} \quad m_{N,i} = \frac{y_{x,i}}{\sqrt{2}} w, \tag{A6}$$

and θ_s, m_h, m_s correspond to Eqs. (8)–(10). The loop functions A_0 and B_0 are given as

$$A_0(m^2) = m^2\left(1 - \ln\left(\frac{m^2}{\mu^2}\right)\right), \tag{A7}$$

$$B_0(s, m_1^2, m_2^2) = -\int_0^1 \mathrm{d}u \ln\left(\frac{u m_1^2 + (1-u)m_2^2 - u(1-u)s}{\mu^2}\right). \tag{A8}$$

In the special case of vanishing masses, the latter reduces to

$$B_0(s,0,0) = 2 - \ln\left(-\frac{s}{\mu^2}\right) = 2 - \ln\left|\frac{s}{\mu^2}\right| + \mathrm{i}\pi\Theta(s) \tag{A9}$$

where Θ is the Heaviside step function.

APPENDIX B: ONE-LOOP CORRECTIONS TO GAUGE BOSONS AND ELECTROWEAK INPUT PARAMETERS IN THE SWSM

The SWSM introduces new corrections to the W and Z gauge boson self-energies. The radiative corrections from the new gauge sector are neglected due to coupling suppression $g_z \lesssim 10^{-4}$, whereas the sterile neutrinos may contribute radiatively through the PMNS matrix as well as at tree level by affecting the Fermi coupling G_{F} through the low-energy muon decay. We neglect the neutrino contributions (to be investigated in an upcoming paper) and focus here on the pure scalar radiative corrections. In the $\overline{\mathrm{MS}}$ scheme the scalar SW contribution to the gauge boson self-energies is

$$\Pi_{VV}^{\mathrm{SW}}(p^2) = \frac{\sin^2\theta_s}{16\pi^2}\frac{m_V^2}{v^2}\left(F(p^2, m_V^2, m_s^2) - F(p^2, m_V^2, m_h^2)\right), \quad V = W, Z, \tag{B1}$$

where the loop function F is defined as

$$F(s, m_1^2, m_2^2) = \frac{2}{3}\left(m_1^2 + m_2^2 - \frac{s}{3}\right) + \left(\frac{s + m_1^2 - m_2^2}{3s}\right)\left(A_0(m_1^2) - A_0(m_2^2)\right) - \frac{1}{3}A_0(m_2^2) - \frac{1}{3}\left(\frac{(m_1^2 - m_2^2)^2}{s} - 2(m_2^2 - 5m_1^2) + s\right) \times B_0(s, m_1^2, m_2^2). \tag{B2}$$

We have checked, in the R_ξ gauge, that the scalar contribution $\Pi_{VV}^{\mathrm{SW}}(p^2)$ is explicitly independent of the gauge parameter ξ, hence gauge invariant. Furthermore, $\Pi_{VV}^{\mathrm{SW}}(M_V^2)$ is independent of the renormalization scale at one-loop accuracy.

The shift in the electroweak input parameters due to the SW corrections is then

$$\frac{\delta g_{\mathrm{L}}}{g_{\mathrm{L}}} = \frac{1}{4m_W^2 - 2m_Z^2}\left(\Pi_{WW}^{\mathrm{SW}}(0) - \frac{m_W^2}{m_Z^2}\Pi_{ZZ}^{\mathrm{SW}}(M_Z^2)\right), \tag{B3}$$

$$\frac{\delta g_Y}{g_Y} = \frac{m_Z^2 - m_W^2}{4m_W^2 - 2m_Z^2}\left(-\frac{\Pi_{WW}^{\mathrm{SW}}(0)}{m_W^2} + \frac{\Pi_{ZZ}^{\mathrm{SW}}(M_Z^2)}{m_Z^2}\right), \tag{B4}$$

$$\frac{\delta v}{v} = -\frac{\Pi_{WW}^{\mathrm{SW}}(0)}{2m_W^2}, \tag{B5}$$

which agrees with Eq. (22) of [20]. The W-boson pole mass is then given as

$$M_W{}^2 = \frac{1}{4}(g_{\mathrm{L}} + \delta g_{\mathrm{L}})^2 (v + \delta v)^2 + \Pi_{WW}^{\mathrm{SM}}(M_W{}^2) + \Pi_{WW}^{\mathrm{SW}}(M_W{}^2). \tag{B6}$$

It is convenient to express M_W as the sum of the SM M_W^{theo} and the new physics contribution δM_W as

$$M_W = M_W^{\mathrm{theo.}} + \delta M_W, \quad \text{with}$$
$$\delta M_W = M_W \frac{\delta v}{v} + \frac{1}{2}\delta g_{\mathrm{L}} v + \frac{\Pi_{WW}^{\mathrm{SW}}(M_W)}{2M_W}. \tag{B7}$$

[1] Y. Fukuda *et al.* (Super-Kamiokande Collaboration), Evidence for Oscillation of Atmospheric Neutrinos, Phys. Rev. Lett. **81**, 1562 (1998).

[2] Q. R. Ahmad *et al.* (SNO Collaboration Collaboration), Measurement of the Rate of $\nu_e + d \to p + p + e^-$ Interactions Produced by ^8b Solar Neutrinos at the Sudbury Neutrino Observatory, Phys. Rev. Lett. **87**, 071301 (2001).

[3] F. Bezrukov, M. Y. Kalmykov, B. A. Kniehl, and M. Shaposhnikov, Higgs boson mass and new physics, J. High Energy Phys. 10 (2012) 140.

[4] G. Degrassi, S. Di Vita, J. Elias-Miro, J. R. Espinosa, G. F. Giudice, G. Isidori, and A. Strumia, Higgs mass and vacuum stability in the Standard Model at NNLO, J. High Energy Phys. 08 (2012) 098.

[5] D. Buttazzo, G. Degrassi, P. P. Giardino, G. F. Giudice, F. Sala, A. Salvio, and A. Strumia, Investigating the near-criticality of the Higgs boson, J. High Energy Phys. 12 (2013) 089.

[6] A. V. Bednyakov, B. A. Kniehl, A. F. Pikelner, and O. L. Veretin, Stability of the Electroweak Vacuum: Gauge Independence and Advanced Precision, Phys. Rev. Lett. **115**, 201802 (2015).

[7] G. Hinshaw *et al.* (WMAP Collaboration), Nine-year Wilkinson Microwave Anisotropy Probe (WMAP) observations: Cosmological parameter results, Astrophys. J. Suppl. Ser. **208**, 19 (2013).

[8] N. Aghanim *et al.* (Planck Collaboration), Planck 2018 results. VI. Cosmological parameters, Astron. Astrophys. **641**, A6 (2020).

[9] D. J. Eisenstein *et al.* (SDSS Collaboration), Detection of the baryon acoustic peak in the large-scale correlation function of SDSS luminous red galaxies, Astrophys. J. **633**, 560 (2005).

[10] Y. Sofue and V. Rubin, Rotation curves of spiral galaxies, Annu. Rev. Astron. Astrophys. **39**, 137 (2001).

[11] M. Bartelmann and P. Schneider, Weak gravitational lensing, Phys. Rep. **340**, 291 (2001).

[12] T. Aoyama *et al.*, The anomalous magnetic moment of the muon in the Standard Model, Phys. Rep. **887**, 1 (2020).

[13] G. W. Bennett *et al.* (Muon g-2 Collaboration), Final report of the muon E821 anomalous magnetic moment measurement at BNL, Phys. Rev. D **73**, 072003 (2006).

[14] B. Abi *et al.* (Muon g-2 Collaboration), Measurement of the Positive Muon Anomalous Magnetic Moment to 0.46 ppm, Phys. Rev. Lett. **126**, 141801 (2021).

[15] S. Borsanyi *et al.*, Leading hadronic contribution to the muon magnetic moment from lattice QCD, Nature (London) **593**, 51 (2021).

[16] B. Holdom, Two U(1)'s and ϵ charge shifts, Phys. Lett. **166B**, 196 (1986).

[17] M. Pospelov, A. Ritz, and M. B. Voloshin, Secluded WIMP dark matter, Phys. Lett. B **662**, 53 (2008).

[18] R. M. Schabinger and J. D. Wells, A minimal spontaneously broken hidden sector and its impact on Higgs boson physics at the Large Hadron Collider, Phys. Rev. D **72**, 093007 (2005).

[19] B. Patt and F. Wilczek, Higgs-field portal into hidden sectors, arXiv:0605188.

[20] A. Falkowski, C. Gross, and O. Lebedev, A second Higgs from the Higgs portal, J. High Energy Phys. 05 (2015) 057.

[21] M. Lindner, D. Schmidt, and A. Watanabe, Dark matter and U(1)′ symmetry for the right-handed neutrinos, Phys. Rev. D **89**, 013007 (2014).

[22] https://atlas.web.cern.ch/Atlas/GROUPS/PHYSICS/PUBNOTES/ATL-PHYS-PUB-2021-019/.

[23] http://cms-results.web.cern.ch/cms-results/public-results/publications/SUS/SUS.html.

[24] B. Grzadkowski, M. Iskrzynski, M. Misiak, and J. Rosiek, Dimension-six terms in the standard model Lagrangian, J. High Energy Phys. 10 (2010) 085.

[25] Z. Trócsányi, Super-weak force and neutrino masses, Symmetry **12**, 107 (2020).

[26] S. Iwamoto, T. J. Kärkkäinen, Z. Péli, and Z. Trócsányi, One-loop corrections to light neutrino masses in gauged U(1) extensions of the standard model, Phys. Rev. D **104**, 055042 (2021).

[27] S. Iwamoto, K. Seller, and Z. Trócsányi, Sterile neutrino dark matter in a U(1) extension of the standard model, J. Cosmol. Astropart. Phys. 01 (2022) 035.

[28] Z. Péli, I. Nándori, and Z. Trócsányi, Particle physics model of curvaton inflation in a stable universe, Phys. Rev. D **101**, 063533 (2020).

[29] We denote the pole mass of a particle p as M_p.

[30] P. A. Zyla *et al.* (Particle Data Group), Review of particle physics, Prog. Theor. Exp. Phys. **2020**, 083C01 (2020).

[31] D. Banerjee *et al.* (NA64 Collaboration), Dark Matter Search in Missing Energy Events with NA64, Phys. Rev. Lett. **123**, 121801 (2019).

[32] W. Porod, SPheno, a program for calculating supersymmetric spectra, SUSY particle decays and SUSY particle production at e^+e^- colliders, Comput. Phys. Commun. **153**, 275 (2003).

[33] W. Porod and F. Staub, SPheno 3.1: Extensions including flavour, *CP*-phases and models beyond the MSSM, Comput. Phys. Commun. **183**, 2458 (2012).

[34] There is a price to pay for this speedup; namely, we discard small portions of the parameter space, where $w^{(1)}(M_t)$ is not positive but $w^{(2)}(M_t)$ is.

[35] J. Elias-Miró, J. R. Espinosa, G. F. Giudice, H. M. Lee, and A. Strumia, Stabilization of the electroweak vacuum by a scalar threshold effect, J. High Energy Phys. 06 (2012) 031.

[36] J. de Blas, M. Ciuchini, E. Franco, A. Goncalves, S. Mishima, M. Pierini, L. Reina, and L. Silvestrini, Global analysis of electroweak data in the Standard Model, Phys. Rev. D **106**, 033003 (2022).

[37] T. Robens and T. Stefaniak, Status of the Higgs singlet extension of the standard model after LHC run 1, Eur. Phys. J. C **75**, 104 (2015).

[38] T. Robens, Constraining extended scalar sectors at current and future colliders, in *Proceedings of the 21st Hellenic School and Workshops on Elementary Particle Physics and Gravity* (2022), arXiv:2203.17016.

[39] We leave the complete analysis to a forthcoming study.

[40] M. Baak, M. Goebel, J. Haller, A. Hoecker, D. Kennedy, R. Kogler, K. Moenig, M. Schott, and J. Stelzer, The electroweak fit of the standard model after the discovery of a new boson at the LHC, Eur. Phys. J. C **72**, 2205 (2012).

[41] M. Ciuchini, E. Franco, S. Mishima, and L. Silvestrini, Electroweak precision observables, new physics and the

nature of a 126 GeV Higgs boson, J. High Energy Phys. 08 (2013) 106.
[42] G. Degrassi, P. Gambino, and P. P. Giardino, The $m_w - m_z$ interdependence in the standard model: A new scrutiny, J. High Energy Phys. 05 (2015) 154.
[43] E. Fernandez-Martinez, J. Hernandez-Garcia, and J. Lopez-Pavon, Global constraints on heavy neutrino mixing, J. High Energy Phys. 08 (2016) 033.
[44] M. Blennow, P. Coloma, E. Fernández-Martínez, and M. González-López, Right-handed neutrinos and the CDF II anomaly, arXiv:2204.04559.
[45] D. López-Val and T. Robens, Δr and the W-boson mass in the singlet extension of the standard model, Phys. Rev. D **90**, 114018 (2014).
[46] T. Aaltonen *et al.* (CDF Collaboration), High-precision measurement of the *W* boson mass with the CDF II detector, Science **376**, 170 (2022).
[47] Recently, we became aware of Ref. [48] where the effect of the singlet scalar extension of the SM on the mass of the *W* boson was investigated in light of the CDF-II result.
[48] K. Sakurai, F. Takahashi, and W. Yin, Singlet extensions and W boson mass in the light of the CDF II result, Phys. Lett. B **833**, 137324 (2022).
[49] The complete analysis is left for future study.
[50] We postpone the check of the dependence of the exclusion bands on $\lambda(M_t)$ as it is not expected to be significant.
[51] S. von Buddenbrock, N. Chakrabarty, A. S. Cornell, D. Kar, M. Kumar, T. Mandal, B. Mellado, B. Mukhopadhyaya, R. G. Reed, and X. Ruan, Phenomenological signatures of additional scalar bosons at the LHC, Eur. Phys. J. C **76**, 580 (2016).
[52] A. Crivellin, Y. Fang, O. Fischer, A. Kumar, M. Kumar, E. Malwa, B. Mellado, N. Rapheeha, X. Ruan, and Q. Sha, Accumulating evidence for the associate production of a neutral scalar with mass around 151 GeV, arXiv:2109.02650.